

# SEQR: SECURE AND EFFICIENT QR-BASED LoRA ROUTING

## Anonymous authors

Paper under double-blind review

## ABSTRACT

Low-Rank Adaptation (LoRA) has become a standard technique for parameter-efficient fine-tuning of large language models, enabling large libraries of LoRAs, each for a specific task or domain. Efficiently selecting the correct LoRA adapter for a given input remains a challenge, particularly in secure environments where supervised training of routers may raise privacy concerns. Motivated by previous approaches, we formalize the goal of unsupervised LoRA routing in terms of activation norm maximization, providing a theoretical framework for analysis. We demonstrate the discriminative power of activation norms and introduce SEQR, an unsupervised LoRA routing algorithm designed to maximize efficiency while providing strict routing guarantees. SEQR provably identifies the norm-maximizing adapter with significantly greater efficiency, making it a highly scalable and effective solution for dynamic LoRA composition. We validate our results through experiments that demonstrate improved multi-task performance and efficiency. <sup>1</sup>

## 1 INTRODUCTION

Language model users can benefit from fine-tuning existing models on custom data, but may be constrained by security policies surrounding data access control or retention (Fleshman et al., 2024; Shi et al., 2025). Low-Rank Adaptation (LoRA) (Hu et al., 2022) is a popular parameter-efficient technique for fine-tuning these models. Widely-used software packages, such as `peft` (Mangrulkar et al., 2022), and model repositories, such as *huggingface* (Wolf et al., 2020), have contributed to the proliferation of LoRA-based experts fine-tuned for various tasks or data domains (Brüel-Gabrielsson et al., 2024; Huang et al., 2024). The broad deployment of language models has led to techniques for securing and controlling training data (Fleshman et al., 2024; Chowdhury et al., 2025; Shi et al., 2025). For example, ADAPTERSWAP leverages LoRA adapters to segment data into separate parameter groups, enabling user-based access control at the model level (Fleshman et al., 2024). The authorized LoRAs for a particular user can then be applied to the model at inference time, and adapters can be quickly retrained if training data is later removed to meet retention policies (Fleshman et al., 2024).

Naively applying all authorized LoRAs to a model can lead to parameter interference, significantly reducing the model performance (Wortsman et al., 2022; Chronopoulou et al., 2023; Ilharco et al., 2023; Fleshman et al., 2024). Numerous model merging strategies have been developed to address this challenge (Ortiz-Jimenez et al., 2023; Yadav et al., 2023; Tang et al., 2024; Yu et al., 2024; Stoica et al., 2025). Alternatively, LoRAs for the same model can be treated as a *mixture-of-experts* (Jacobs et al., 1991; Fedus et al., 2022) by learning to route inputs to a smaller set of appropriate adapters (Pfeiffer et al., 2021; Wang et al., 2022; Caccia et al., 2023; Ponti et al., 2023; Fleshman et al., 2024; Huang et al., 2024; Zadouri et al., 2024). Multi-LoRA frameworks have also been used for federated learning, where LoRA training dynamics suggest that the LoRA  $A$  matrices learn global features which can be shared among the different adapters (Sun et al., 2024b; Guo et al., 2025).

Supervised training of a router using data across protected silos is not an option in strict data security scenarios, as adversarial techniques exist for leaking information related to the data (Shokri et al., 2017; Carlini et al., 2022; Yao, 2024; Zhou et al., 2025). Recent approaches perform LoRA routing in an unsupervised manner by selecting adapters for a given input without any router training or cross-silo data requirements (Ostapenko et al., 2024; Fleshman & Van Durme, 2025a;b). In this work,

<sup>1</sup>Code available at <https://anonymous.4open.science/r/SEQR>

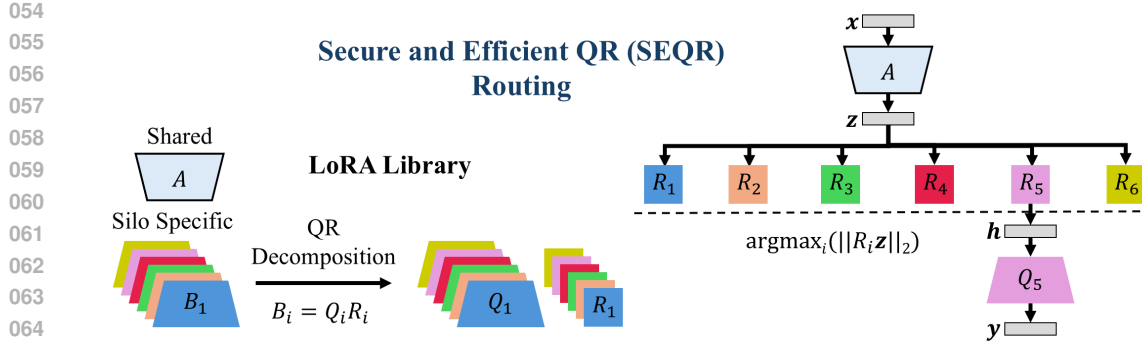


Figure 1: Secure and Efficient QR (SEQR) routing: Rank- $r$  LoRAs are trained on multiple datasets using a shared  $A$  matrix frozen at initialization. Each  $B_i$  is stored in terms of its QR decomposition. During inference, input vectors are routed efficiently using the smaller  $r \times r$  matrices.

we formalize the goal of these techniques and analyze their routing procedures. We introduce a new method, SEQR (Figure 1), which is more efficient than previous approaches while providing strict routing guarantees. Specifically we:

- Formalize unsupervised LoRA routing as activation norm-maximization;
- Provide theoretical results for current approaches under this framework;
- Introduce a more efficient routing scheme, SEQR, which provably selects the norm-maximizing adapter; and
- Perform empirical experiments demonstrating the benefits of our approach.

## 2 BACKGROUND AND RELATED WORK

### 2.1 LORA

LoRA updates the pretrained layer weights  $W_0 \in \mathbb{R}^{m \times n}$  by freezing the existing weights and injecting two low-rank matrices of learnable parameters  $A \in \mathbb{R}^{r \times n}$  and  $B \in \mathbb{R}^{m \times r}$  such that the new weights are  $W = W_0 + BA$ , with a small rank  $r \ll \min(m, n)$  that considerably reduces the number of trainable parameters (Hu et al., 2022). For an input vector  $\mathbf{x} \in \mathbb{R}^n$ , the output  $\mathbf{y} \in \mathbb{R}^m$  can be computed directly with the new weights as  $\mathbf{y} = W\mathbf{x}$  or separately as  $\mathbf{y} = W_0\mathbf{x} + B\mathbf{A}\mathbf{x}$ . LoRA fine-tuning has been widely adopted, and the success has led to many extensions to the original idea (Zhang et al., 2023b; Albert et al., 2024; Buehler & Buehler, 2024; Kopitzko et al., 2024; Li et al., 2024; Liu et al., 2024a; Bini et al., 2025). LoRA merging or routing is necessary in the case where many LoRAs are trained on different groups of data, resulting in a set of available LoRAs  $\mathcal{A} = \{B_1 A_1, B_2 A_2, \dots, B_N A_N\}$  for each adapted layer of the model. Various techniques for merging LoRAs into a single update have been developed, but merging suffers from parameter interference when the number of adapters is large (Ortiz-Jimenez et al., 2023; Yadav et al., 2023; Tang et al., 2024; Yu et al., 2024; Stoica et al., 2025). The goal of unsupervised LoRA routing is to choose the subset of adapters best suited for each vector in a sequence, without explicitly training a router (Ostapenko et al., 2024; Fleshman & Van Durme, 2025b;a). These approaches alleviate parameter interference while providing additional security guarantees (Fleshman & Van Durme, 2025b).

### 2.2 PRIVACY & SECURITY

Organizations may have various security or privacy concerns depending on the data used for training individual LoRAs. Training with differential privacy (DP) provides probabilistic guarantees that an adversary can not infer if particular examples were in the training data (Dwork & Roth, 2014; Abadi et al., 2016). DP can be used to protect user privacy in cases where adversaries may have access to the LoRA weights (Shi et al., 2025). Stricter security requirements incorporate data access control, completely preventing user access to LoRA weights trained on data the user is unauthorized

108 to view (Fleshman et al., 2024). In these cases, training a router to distinguish between LoRAs  
 109 would introduce security concerns, as adversaries with access to the router could potentially leak  
 110 information from the LoRAs themselves (Shokri et al., 2017; Carlini et al., 2022; Yao, 2024; Zhou  
 111 et al., 2025). We focus on the strict security case, where unsupervised routing approaches are needed.  
 112

### 113 2.3 ACTIVATION NORMS

115 Unsupervised LoRA routing can be framed as an *in-distribution* (ID) detection problem, where inputs  
 116 are routed to the adapters trained on data similar to the queries. Prior work has shown that the norm  
 117 of the activation vector produced by model layers can effectively distinguish between in- and out-of  
 118 distribution (OOD) data (Park et al., 2023; Liu et al., 2024b; Shin & Chung, 2024; Sun et al., 2024a;  
 119 Wan et al., 2024). ID data tends to produce large activation spikes in neural networks, including in  
 120 large language models (Sun et al., 2024a). Park et al. (2023) analyze this phenomenon and find that  
 121 the activation norm distinguishes OOD and ID similar to a classifier confidence score. These findings  
 122 justify trying to route to LoRAs which maximize the norm of adapter activations  $\|BAx\|$ .  
 123

### 124 2.4 ARROW ROUTING

125 Ostapenko et al. (2024) use the singular value decomposition (SVD) to convert each LoRA adapter  
 126  $B_i A_i \in \mathcal{A}$  into a product of three matrices with an equivalent product:  
 127

$$B_i A_i = U_i S_i V_i^T, \quad (1)$$

128 where  $U_i \in \mathbb{R}^{m \times r}$  is the orthonormal matrix of left singular vectors,  $S_i \in \mathbb{R}^{r \times r}$  is the diagonal  
 129 matrix of singular values, and  $V_i \in \mathbb{R}^{n \times r}$  is the orthonormal matrix of right singular vectors. ARROW  
 130 routing leverages the fact that the right singular vector  $v_i$  associated with the largest singular value  
 131 corresponds to the direction capturing the most variation in the space of input vectors  $x$  (Ostapenko  
 132 et al., 2024). This *arrow vector*  $v_i$  satisfies  $v_i = \max_{x, \|x\|_2=1} \|B_i A_i x\|_2$ , meaning it maximizes  
 133 the norm of the corresponding adapter activations among unit-length input vectors. We use norm-  
 134 maximization as the explicit goal in this work, allowing for analysis of these approaches. Ostapenko  
 135 et al. (2024) use the set of arrows as prototypes for each of the adapters in  $\mathcal{A}$ , assigning the most weight  
 136 to the adapter corresponding to the arrow satisfying  $\arg\max_i |v_i^T x|$ . The use of vector prototypes  
 137 makes ARROW routing especially efficient, requiring a simple dot product per adapter:  $\mathcal{O}(Nn)$  for  
 138  $N$  adapters with input dimension  $n$ . ARROW routing performs reasonably well, and the authors  
 139 empirically show that the ID adapter tends to produce higher ARROW scores (Ostapenko et al., 2024).  
 140

### 141 2.5 SPECTRAL ROUTING AND LAG

142 SPECTR builds on ARROW by using all right singular vectors to make routing decisions (Fleshman &  
 143 Van Durme, 2025b). Equation 1 is used by SPECTR to convert each adapter into two new matrices:  
 144

$$\hat{B}_i = U_i \quad (2)$$

$$\hat{A}_i = S_i V_i^T, \quad (3)$$

145 such that  $\hat{B}_i \hat{A}_i = B_i A_i$  with  $\hat{A}_i$  now containing the orthogonal directions of maximum variation  
 146 scaled by the singular values. SPECTR generalizes the ARROW scoring method by assigning the  
 147 most weight to the adapter satisfying  $\arg\max_i \|\hat{A}_i x\|_2$ . Computing the SPECTR routing scores is  
 148 less efficient than ARROW:  $\mathcal{O}(Nrn)$ , but SPECTR outperforms ARROW in routing accuracy and  
 149 downstream task performance (Fleshman & Van Durme, 2025b).  
 150

151 LoRA-Augmented Generation (LAG) combines the efficiency of ARROW routing with the improved  
 152 performance of SPECTR by using a two-stage approach (Fleshman & Van Durme, 2025a). First, LAG  
 153 performs top- $k$  filtering using ARROW to reduce the final routing decision to  $k \ll N$  adapters. LAG  
 154 then uses SPECTR to route to the top adapter in the filtered set. Routing complexity is reduced to  
 155  $\mathcal{O}(Nn + krn)$  while still outperforming ARROW (Fleshman & Van Durme, 2025a).  
 156

### 157 2.6 SHARED A

158 While ARROW, SPECTR, and LAG use traditional LoRA fine-tuning, recent work explores a special  
 159 case of LoRA where the  $A$  matrix is frozen at initialization or shared among several LoRAs in a  
 160

federated setting, resulting in similar or improved performance with reduced storage costs (Zhang et al., 2023a; Sun et al., 2024b; Zhu et al., 2024; Guo et al., 2025). Zhu et al. (2024) provides a theoretical analysis showing that the LoRA updates are dominated by the  $B$  matrix during fine-tuning, and that a LoRA with a frozen random  $A$  matrix should perform similarly to one that is fully trained. The asymmetry in training dynamics lends itself to using a global  $A$  matrix and unique  $B$  matrices in multi-LoRA scenarios (Sun et al., 2024b; Guo et al., 2025). We explore this direction in our work, and show that a shared  $A$  matrix allows for more efficient unsupervised LoRA routing techniques.

### 3 THEORETICAL RESULTS AND SEQR

**Problem Statement** We formalize the goal of unsupervised LoRA routing to provide a framework for theoretical analysis. Given the success of using activations for ID/OOD detection and the similar motivation of current unsupervised routing approaches, we propose the following problem:

#### Problem

**LoRA Activation Norm-Maximization.** Given a library of LoRA adapters,  $\mathcal{A} = \{B_1A_1, B_2A_2, \dots, B_NA_N\}$  and an input vector  $\mathbf{x}$ , efficiently find  $\operatorname{argmax}_i \|B_iA_i\mathbf{x}\|_2$ .

We add “efficiently” to the problem statement as an algorithm that simply computes all activation norms directly would be  $\mathcal{O}(Nr(m + n))$ , far worse than current routing approaches. We will demonstrate the discriminative power of LoRA activation norms in Section 4.3.

#### 3.1 ARROW IS NOT NORM-MAXIMIZING

Our first result shows that ARROW is not guaranteed to find the norm-maximizing adapter.

**Theorem 3.1.** *There exists a set of LoRA adapters  $\{B_1A_1, B_2A_2, \dots, B_NA_N\}$  with corresponding arrow vectors  $\{v_1, v_2, \dots, v_N\}$  and  $\mathbf{x} \in \mathbb{R}^n$  where  $\operatorname{argmax}_i |\mathbf{v}_i^T \mathbf{x}| \neq \operatorname{argmax}_i \|B_iA_i\mathbf{x}\|_2$ .*

We provide the proof by construction in Appendix A and confirm with experiments in Section 4.4. The main observation from the proof is that alignment with the top singular vector is not enough to guarantee the adapter will have the largest norm, as misalignment can be overcome with larger singular values. Routing with LAG inherits the lack of guarantee from ARROW, but the top- $k$  selection improves the chances of including the norm-maximizing adapter in the set used for SPECTR selection.

#### 3.2 SPECTR IS NORM-MAXIMIZING

Our next results show that SPECTR scores are equivalent to the activation norms, and therefore SPECTR is norm-maximizing. The proof for Theorem 3.2 is provided in Appendix B.

**Theorem 3.2.** *Let  $B \in \mathbb{R}^{m \times r}$  and  $A \in \mathbb{R}^{r \times n}$  be LoRA matrices with  $\hat{A}$  derived from  $BA$  using Equations 1 and 3, then  $\forall \mathbf{x} \in \mathbb{R}^n$ ,  $\|\hat{A}\mathbf{x}\|_2 = \|BA\mathbf{x}\|_2$ .*

**Corollary 3.2.1.** *Let  $\{B_1A_1, B_2A_2, \dots, B_NA_N\}$  be a set of LoRA adapters converted with Equations 1-3 to the set  $\{\hat{B}_1\hat{A}_1, \hat{B}_2\hat{A}_2, \dots, \hat{B}_N\hat{A}_N\}$ , then  $\operatorname{argmax}_i \|\hat{A}_i\mathbf{x}\|_2 = \operatorname{argmax}_i \|B_iA_i\mathbf{x}\|_2$ .*

These results show that SPECTR provides optimal routing under the stated goal. We are interested in new approaches providing the same guarantee but with improved efficiency.

#### 3.3 SECURE AND EFFICIENT QR (SEQR) ROUTING

Now we explore the special case of our problem statement where all adapters in  $\mathcal{A}$  share the same matrix  $A$ . This matrix is randomly initialized and kept frozen to ensure the same data security provided by other unsupervised routing approaches. For an input  $\mathbf{x}$ , we compute  $\mathbf{z} = A\mathbf{x}$  as an intermediate step. Routing is then required for the set of  $B$  matrices. Directly computing the norm for all would require  $\mathcal{O}(Nmr)$ , which is already equivalent to SPECTR for  $m = n$ . We can improve further by doing a one-time preprocessing step similar to the SVD in ARROW and SPECTR. We precompute the reduced QR decomposition of each  $B_i$ :

$$B_i = Q_i R_i, \quad (4)$$

216 where  $Q_i \in \mathbb{R}^{m \times r}$  is an orthogonal matrix and  $R_i \in \mathbb{R}^{r \times r}$  is upper triangular. Similar to SPECTR,  
 217 we can throw away the original  $B_i$  and store the adapter in this new form. The vector  $\mathbf{z}$  is then routed  
 218 to the adapter satisfying  $\text{argmax}_i \|R_i \mathbf{z}\|_2$ .<sup>2</sup> The routing complexity is only  $\mathcal{O}(Nr^2)$ , which is far  
 219 better than SPECTR and is even more efficient than ARROW routing in the typical LoRA scenario  
 220 where  $r \ll n$ . We restate the complete SEQR routing algorithm in [Appendix F](#). Like SPECTR, we  
 221 show SEQR scores are equivalent to the activation norm for each adapter. Therefore, SEQR always  
 222 selects the norm-maximizing adapter. The proof for Theorem 3.3 is provided in [Appendix C](#).

223 **Theorem 3.3.** *Let  $B \in \mathbb{R}^{m \times r}$  and  $A \in \mathbb{R}^{r \times n}$  be LoRA matrices such that  $B = QR$  from Equation  
 224 4, then  $\forall \mathbf{x} \in \mathbb{R}^n$ ,  $\|RA\mathbf{x}\|_2 = \|BA\mathbf{x}\|_2$ .*

225 **Corollary 3.3.1.** *Let  $\{B_1, B_2, \dots, B_N\}$  be a set of LoRA adapters with a shared  $A$  matrix and  
 226  $\{Q_1R_1, Q_2R_2, \dots, Q_NR_N\}$  from Equation 4, then  $\text{argmax}_i \|R_i A\mathbf{x}\|_2 = \text{argmax}_i \|B_i A_i \mathbf{x}\|_2$ .*

### 228 3.4 ROUTING COMPLEXITY

230 We revisit the routing complexities of ARROW routing, SPECTR, LAG, and SEQR using dimensions  
 231 reported in the LAG experiments for added context ([Fleshman & Van Durme, 2025a](#)). [Table 1](#)  
 232 includes the FLOPs used for routing by each method in this example, including the naive approach  
 233 of computing the norm directly for each adapter. SEQR is two orders of magnitude more efficient  
 234 than any other approach. SEQR also decreases storage costs by offsetting the storage of each  $R_i$  by  
 235 sharing  $A$  across the library. ARROW can also take advantage of improved storage when using a  
 236 shared  $A$  matrix, but arrow vectors require more space than the  $R_i$  matrices when  $n > r^2$ .

237 [Table 1](#): Routing complexity and example FLOPs for each method assuming  $N = 1000$  adapters,  
 238  $n = m = 4096$  hidden dimension,  $k = 20$  LAG filtering, and  $r = 8$  rank adapters.

	Naive	SPECTR	LAG	ARROW	SEQR
<b>FLOPs</b>	66M	33M	5M	4M	<b>64K</b>
<b>Complexity</b>	$\mathcal{O}(Nr(m+n))$	$\mathcal{O}(Nrn)$	$\mathcal{O}(Nn + krn)$	$\mathcal{O}(Nn)$	$\mathcal{O}(Nr^2)$

## 244 4 EXPERIMENTS

245 We conduct experiments to validate our theoretical results and to test whether SEQR provides similar  
 246 or better performance over less efficient alternatives. First, we confirm prior work showing that using  
 247 a fixed  $A$  matrix in LoRA works as well as learning  $A$  individually. We analyze the differences  
 248 in activation norms between these two settings and introduce a calibration step to ensure norms  
 249 between adapters are on the same scale. We measure the ability of each approach to select the  
 250 norm-maximizing adapter and the resulting multi-task performance and efficiency.

### 253 4.1 MODELS AND DATA

254 We first replicate the experiments of [Fleshman & Van Durme \(2025b\)](#) using the Llama-3.2-3B-Instruct  
 255 model ([Grattafiori et al., 2024](#)). We train LoRAs for a variety of tasks: agnews<sup>3</sup>, cola ([Warstadt et al.,  
 256 2019](#)), dbpedia ([Auer et al., 2007](#)), hellaswag ([Zellers et al., 2019](#)), mnli ([Williams et al., 2018](#)),  
 257 mrpc ([Dolan & Brockett, 2005](#)), qnli ([Rajpurkar et al., 2016](#)), qqp,<sup>4</sup> rte ([Wang et al., 2018](#)), and sst2  
 258 ([Socher et al., 2013](#)). Similar to [Ostapenko et al. \(2024\)](#), we subsample the datasets for computational  
 259 feasibility. Using different random seeds, we produce three sets of LoRAs per dataset and category  
 260 (shared vs. unique  $A$  matrix), each trained on 1000 samples from the corresponding dataset. Learning  
 261 rates were optimized per dataset and category but shared across random seeds. All evaluations are  
 262 performed using a held-out set of 1000 examples from each dataset. LoRA  $A$  matrices are initialized  
 263 from  $\mathcal{N}(0, 1/r^2)$  and frozen in the shared setting. The  $B$  matrices are initialized with 0s and trained  
 264 in both cases ([Hu et al., 2022](#)). The complete adapter training details are included in [Appendix D](#).  
 265 Finally, we demonstrate SEQR across different model sizes and families using the Qwen 1.5B, Llama  
 266 3B, Qwen 7B, and Llama 8B instruct models ([Grattafiori et al., 2024; Qwen et al., 2025](#)).

267 <sup>2</sup>We z-score these raw scores based on our findings in [Section 4.3](#).

268 <sup>3</sup>[http://groups.di.unipi.it/~gulli/AG\\_corpus\\_of\\_news\\_articles.html](http://groups.di.unipi.it/~gulli/AG_corpus_of_news_articles.html)

269 <sup>4</sup><https://quoradata.quora.com/First-Quora-Dataset-Release-Question-Pairs>

270 Table 2: Accuracy of Llama-3B LoRAs using a unique or fixed  $A$  matrix shared across datasets.  
271

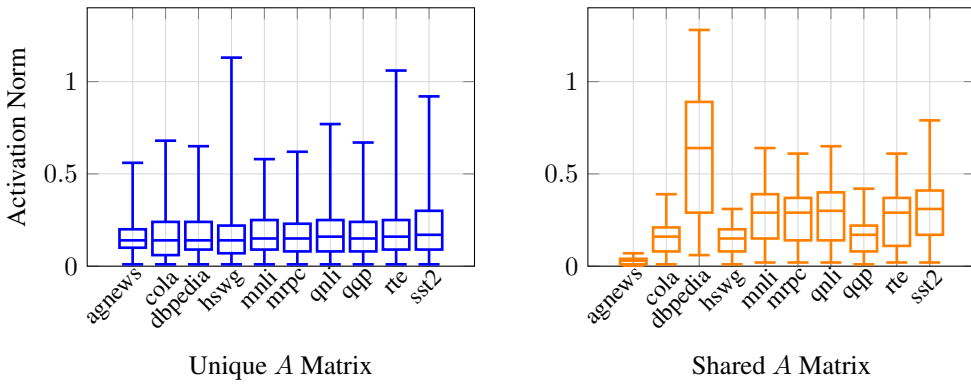
	agnews	cola	dbped	hswag	mnli	mrpc	qnli	qqp	rte	sst2	AVG
Unique	90.4	78.8	98.7	83.6	86.1	84.7	84.9	86.5	88.2	92.4	87.4
Shared	90.0	78.9	99.0	81.5	85.7	85.0	85.5	86.3	87.9	92.8	87.3

275  
276 4.2 UNIQUE VS. SHARED  
277

278 Before measuring routing performance, we ensure that using frozen  $A$  matrices results in similar  
279 LoRA performance. Table 2 shows the accuracy of each adapter on its corresponding test set, averaged  
280 across three initializations. Accuracy is within 1% between the two categories in most cases, with  
281 the largest deviation being a 2% difference on hellaswag when using the frozen  $A$  matrices. Overall,  
282 the average performance is nearly identical, a finding consistent with prior work showing similar  
283 performance with a frozen  $A$  (Zhang et al., 2023a; Sun et al., 2024b; Zhu et al., 2024).

284  
285 4.3 ACTIVATION NORMS  
286

287 Activation norms of a given adapter can be informative for distinguishing ID from OOD data.  
288 However, to ensure bias-free routing, these norms must be comparable across adapters. For instance,  
289 the agnews adapter may produce lower norms than the cola adapter regardless of the dataset, even if  
290 it generates higher norms on agnews data specifically. In such cases, the routing procedure would be  
291 biased toward selecting the cola adapter. We explore and mitigate this potential bias in norms.

304  
305 Figure 2: Distribution of average activation norms for each dataset when using LoRA adapters with  
306 unique  $A$  matrices or a fixed  $A$  matrix shared across adapters.

307 We gather the average activation norms across model layers for each adapter in Figure 2. We find  
308 that the activation norms are very consistent across adapters when using LoRAs trained with unique  
309  $A$  matrices. However, when the adapters share a frozen  $A$  matrix across datasets, the variance  
310 in activation norms is considerable. To address the issue, we introduce an offline calibration step  
311 for the norm-based approaches. We compute the mean,  $\mu_i$ , and standard deviation,  $\sigma_i$ , of the  
312 activation norm for each adapter using its associated training data. The scores for SPECTR become  
313  $s_i = (\|\hat{A}_i \mathbf{x}\|_2 - \mu_i) / \sigma_i$  and similarly for SEQR  $s_i = (\|R_i A \mathbf{x}\|_2 - \mu_i) / \sigma_i$ , which are the z-scores  
314 of the original raw scores to ensure all adapters are on the same scale. These scores are used in the  
315 final algorithm (Appendix F). ARROW scores remain the same, as  $\mathbf{v}_i$  is unit-length by construction.

316 We visualize the impact of z-scoring by measuring the average activation norm for each adapter, on  
317 each dataset, before and after normalizing the scores (Figure 3). We see that the norms for adapters  
318 with unique  $A$  matrices are already discriminative, but normalizing does sharpen the distribution.  
319 The biased norms in the shared case completely prevent accurate discrimination, with the dbpedia  
320 adapter producing the largest average norm regardless of the dataset. Z-scoring significantly improves  
321 the results, leading to similar relative averages when compared to the traditionally trained LoRAs  
322 with unique  $A$  matrices. The estimated norms could change post-calibration due to noisy estimation  
323 or distribution shift. We measure the sensitivity of performance with respect to these changes in  
Appendix E and find SEQR is robust to relatively large changes in the expected norms.

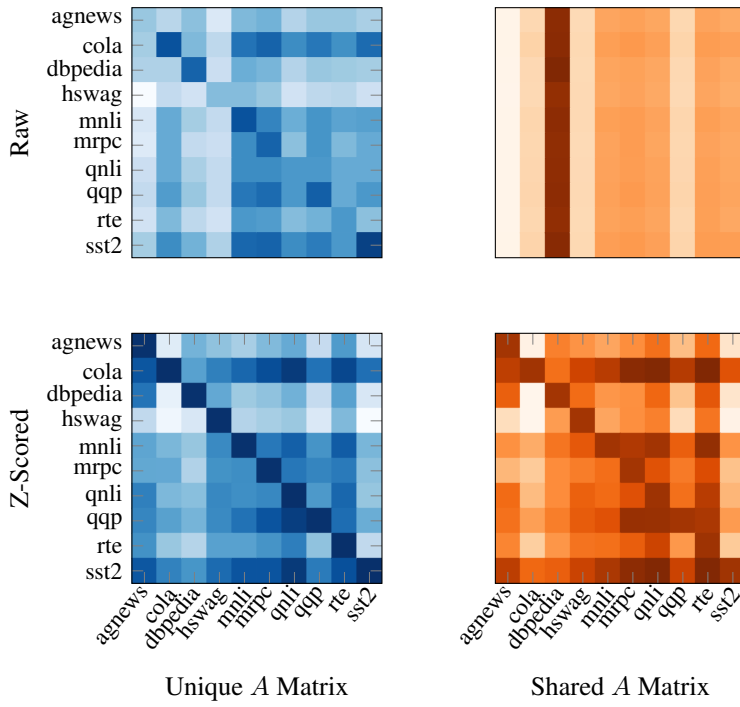


Figure 3: Raw (top) versus z-scored (bottom) activation norms for the adapters using unique (left) or shared (right)  $A$  matrices. Rows are datasets and columns are the applied adapter.

#### 4.4 ROUTING ACCURACY

We validate our theoretical results by measuring the percentage of tokens routed to the norm-maximizing adapter (Figure 4). ARROW chooses the adapter with the top singular vector most aligned to the input. This adapter is the norm-maximizing adapter for only 16% of tokens. The routing accuracy of LAG scales almost linearly with  $k$ , as LAG is equivalent to ARROW at  $k = 1$  and equivalent to SPECTR at  $k = 10$ . SPECTR and SEQR both choose the norm-maximizing adapter in all cases. These results empirically confirm our theoretical findings and are consistent with prior work showing ARROW routing accuracies just above random chance and improved routing with SPECTR (Fleshman & Van Durme, 2025b).

#### 4.5 TASK PERFORMANCE

We measure multi-task performance by evaluating the routing methods on the withheld data from each dataset. Keeping with previous work, we include MU-routing as an additional baseline (Ostapenko et al., 2024; Fleshman & Van Durme, 2025b). MU forgoes routing to individual LoRAs and instead computes the mean update using all adapters:  $\mathbf{y} = \mathbf{W}\mathbf{x} + \frac{1}{N} \sum_{i=1}^N \mathbf{B}_i \mathbf{A}\mathbf{x}$ . While simple, averaging adapters can lead to poor performance due to interference in parameter space, especially with a large number of adapters (Ortiz-Jimenez et al., 2023; Tang et al., 2024; Stoica et al., 2025).

Fleshman & Van Durme (2025a) use  $k = 20$  with LAG, filtering their adapter library to 2% of the total before using SPECTR to make the final selection. With only 10 adapters, we use a 30% reduction with  $k = 3$  for demonstration purposes, but note the LAG task performance is equivalent to ARROW

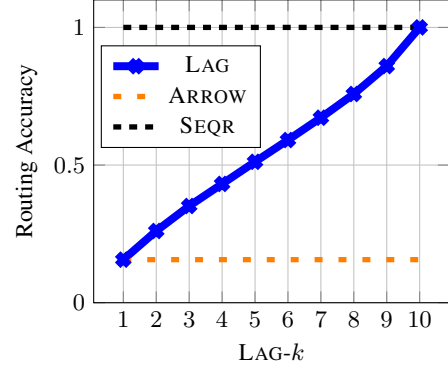


Figure 4: Routing accuracy as  $k$  increases for LAG. LAG is equivalent to ARROW at  $k = 1$  and to SPECTR at  $k = 10$ . ARROW chooses the norm-maximizing adapter for 16% of tokens.

378 Table 3: Mean and standard deviation of performance achieved across datasets and routing methods.  
 379 SPECTR achieves identical performance as SEQR but at a higher computational cost.  
 380

		agnw	cola	dbpd	hswg	mnli	mrpc	qnli	qqp	rte	sst2	AVG
381 Qwen-1.5B	MU	77 ±0.3	93 ±0.3	94 ±0.1	52 ±0.7	73 ±0.0	85 ±0.1	94 ±0.3	95 ±0.4	93 ±0.1	93 ±0.5	84.8
	ARW	98 ±0.7	<b>97</b> ±0.6	<b>99</b> ±0.0	94 ±0.5	<b>77</b> ±2.2	93 ±1.2	96 ±1.3	98 ±1.0	97 ±1.2	98 ±1.5	94.8
	LAG	99 ±0.3	96 ±2.3	<b>99</b> ±0.8	93 ±0.7	75 ±0.7	93 ±0.4	<b>97</b> ±0.1	98 ±1.1	98 ±0.7	<b>99</b> ±1.1	94.8
	SQR	<b>100</b> ±0.3	96 ±1.8	<b>99</b> ±1.0	<b>95</b> ±0.9	75 ±0.1	<b>94</b> ±1.0	<b>97</b> ±0.5	<b>99</b> ±0.7	<b>99</b> ±0.4	<b>99</b> ±0.3	<b>95.1</b>
	MU	16 ±9.7	86 ±3.6	89 ±2.6	53 ±0.0	48 ±2.5	76 ±4.5	79 ±0.6	61 ±4.4	73 ±1.1	94 ±0.3	67.5
	ARW	89 ±0.9	92 ±1.6	<b>100</b> ±0.1	78 ±12.2	78 ±2.1	92 ±1.2	92 ±2.8	<b>97</b> ±0.9	94 ±3.1	97 ±1.0	90.9
389 Llama-3B	LAG	89 ±1.0	94 ±0.8	<b>100</b> ±0.2	86 ±2.1	<b>81</b> ±6.2	<b>93</b> ±1.5	95 ±0.9	<b>97</b> ±0.2	<b>96</b> ±1.5	<b>98</b> ±0.9	92.9
	SQR	<b>91</b> ±0.5	<b>96</b> ±0.9	<b>100</b> ±0.2	<b>87</b> ±2.3	<b>81</b> ±7.5	<b>93</b> ±2.2	<b>96</b> ±1.4	<b>97</b> ±0.1	<b>96</b> ±2.1	<b>98</b> ±2.3	<b>93.5</b>
	MU	91 ±0.2	95 ±0.1	99 ±0.0	88 ±0.3	77 ±0.4	69 ±0.8	73 ±0.6	91 ±0.5	90 ±0.3	95 ±0.2	86.8
	ARW	<b>100</b> ±0.2	98 ±1.2	<b>100</b> ±0.2	<b>100</b> ±0.5	97 ±0.5	95 ±1.4	96 ±0.4	<b>99</b> ±0.1	<b>98</b> ±0.1	<b>99</b> ±0.4	98.1
395 Qwen-7B	LAG	<b>100</b> ±0.3	98 ±0.8	<b>100</b> ±0.1	<b>100</b> ±0.5	97 ±0.4	96 ±1.2	<b>97</b> ±0.4	97 ±0.2	97 ±0.5	<b>99</b> ±0.3	98.5
	SQR	<b>100</b> ±0.1	<b>99</b> ±0.6	<b>100</b> ±0.1	<b>100</b> ±0.6	<b>98</b> ±0.8	<b>98</b> ±0.9	<b>97</b> ±0.8	<b>99</b> ±0.3	<b>97</b> ±0.3	<b>99</b> ±0.2	<b>98.7</b>
	MU	0 ±0.1	88 ±8.9	34 ±13.9	66 ±0.7	66 ±0.8	84 ±0.8	83 ±3.7	64 ±7.4	70 ±20.5	49 ±27.8	60.4
	ARW	98 ±0.4	96 ±0.4	<b>99</b> ±0.2	98 ±0.7	<b>92</b> ±1.8	94 ±1.2	97 ±1.8	<b>98</b> ±0.4	95 ±0.1	<b>98</b> ±0.2	96.5
402 Llama-8B	LAG	<b>99</b> ±0.4	97 ±0.8	98 ±0.7	<b>99</b> ±0.6	91 ±0.9	<b>95</b> ±1.3	97 ±1.6	<b>98</b> ±0.4	97 ±0.6	<b>98</b> ±0.5	96.8
	SQR	<b>99</b> ±0.6	<b>98</b> ±0.5	<b>99</b> ±0.6	<b>99</b> ±1.0	91 ±0.5	<b>95</b> ±1.2	<b>98</b> ±0.7	<b>98</b> ±0.3	<b>98</b> ±0.8	<b>98</b> ±0.6	<b>97.2</b>

409  
 410 for  $k = 1$  and to SPECTR and SEQR at  $k = 10$ . We control for variation in task difficulty by dividing  
 411 each score by the performance of the correct adapter (Ostapenko et al., 2024; Fleshman & Van Durme,  
 412 2025b). This normalization captures the percentage of the upper bound performance achieved by  
 413 routing with a perfect oracle. The oracle scores are included in Appendix G. We report the mean  
 414 performance and standard deviation over three random seeds in Table 3. SEQR and SPECTR route  
 415 equivalently, so we only include SEQR in the table. SEQR achieves the highest average score in all  
 416 cases, outperforming MU, ARROW, and LAG.<sup>5</sup> The similar task-performance with LAG and identical  
 417 performance with SPECTR make differences in efficiency a primary consideration for choosing  
 418 among the various approaches. Next, we explore these differences in more detail.  
 419

#### 420 4.6 ROUTING EFFICIENCY

421  
 422 SEQR yields the same improved multi-task performance as SPECTR, but with far greater efficiency.  
 423 We measure the realized FLOPs and peak GPU memory used by each approach under various  
 424 conditions (Figure 5). Total memory usage is dominated by the storage of the adapter library, so  
 425 SEQR and ARROW are around twice as efficient when using shared  $A$  matrices. SPECTR and LAG  
 426 require storing unique  $\hat{A}_i$  matrices per adapter, even when the original  $A$  matrix is shared. SEQR  
 427 stores an extra  $Nr^2$  parameters for the  $R_i$  matrices while ARROW stores an extra  $Nn$  for the arrow  
 428 vectors. This gives SEQR an additional advantage in storage costs when  $r^2 < n$ . For computation,  
 429 SEQR provides a significant reduction in FLOPs over other methods, especially for large adapter  
 430 libraries using a smaller LoRA rank per adapter. ARROW requires fewer FLOPs than SEQR when  
 431

<sup>5</sup>A paired t-test produces  $p = 3.78e^{-4}$  when comparing with ARROW and  $p = 3.7e^{-5}$  with LAG.

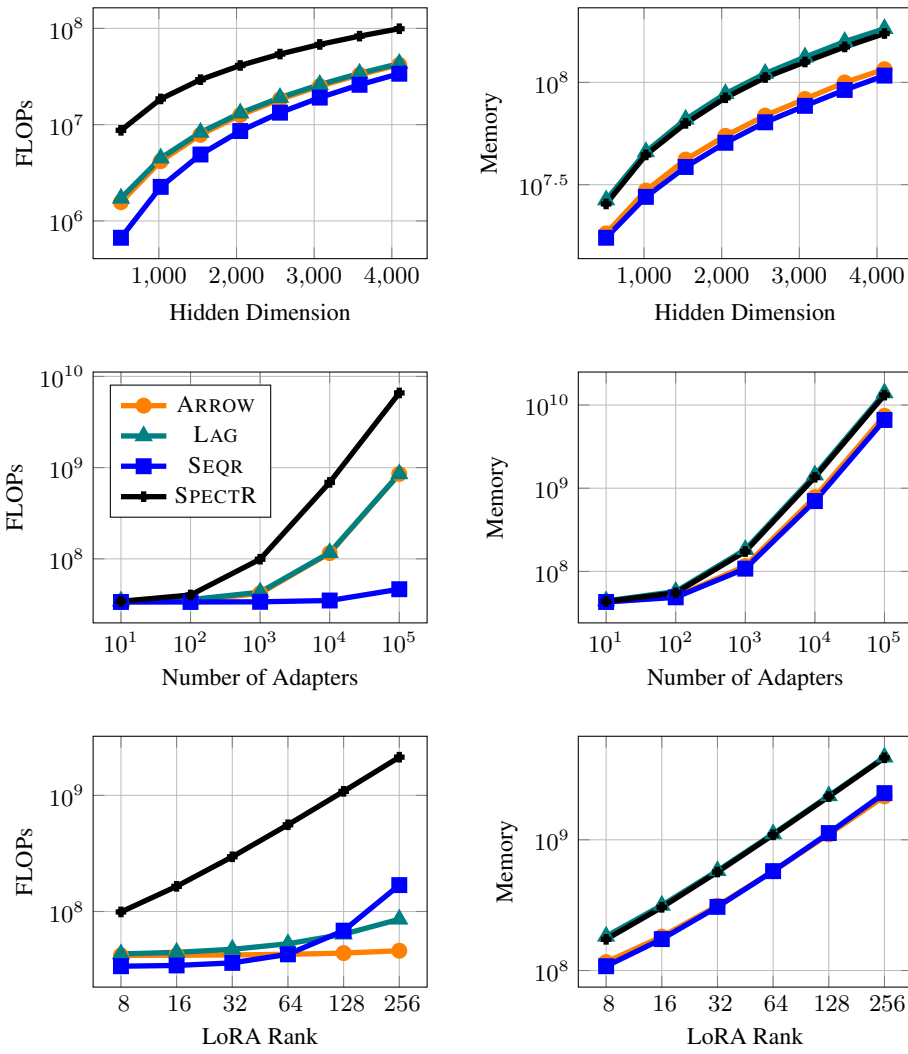


Figure 5: FLOPs (left) and GPU bytes used (right) for each method while varying hidden dimension (top), number of adapters in library (middle), and LoRA rank (bottom). Settings are fixed to  $n = 4096$ ,  $N = 1,000$ , and  $r = 8$  when not under evaluation. LAG uses  $k = 20$  for ARROW filtering.

$r > \sqrt{n}$ , but the relative task-performance of ARROW degrades at higher rank, where routing decisions are still limited by the rank-1 prototypes (Fleshman & Van Durme, 2025b).

## 5 CONCLUSION

In conclusion, we introduced SEQR, a state-of-the-art unsupervised LoRA routing algorithm. We formalized the goal of unsupervised LoRA routing in terms of activation norm-maximization and provided theoretical results for previous routing methods under this framework. The approaches that guarantee selecting the norm-maximizing adapter had better multi-task performance in our experiments. We showed that SEQR has this guarantee while being orders of magnitude more efficient than existing alternatives. SEQR leverages prior work showing that similar performance can be achieved when using LoRAs with frozen  $A$  matrices shared across adapters, a finding we empirically validate. Sharing the  $A$  matrices resulted in a higher variance in activation norms, which we corrected via an offline calibration step. Calibration improved performance for SPECTR and SEQR, with SEQR being significantly faster in execution due to the increased efficiency. SEQR maintains the security benefits of other unsupervised methods, preventing data leakage without access to the LoRA weights.

486 

## 6 REPRODUCIBILITY

488 We take several steps to ensure the reproducibility of our work. First, we provide our source code  
 489 containing the functionality for producing our exact training datasets, random seeds, adapter training,  
 490 and evaluation. We provide similar details in Section 4.1 and Appendix D. Our theoretical results  
 491 contain step-by-step proofs in Appendix A, Appendix B and Appendix C. Finally, we provide a  
 492 concise version of our new routing procedure in Appendix F.

494 

## REFERENCES

496 Martin Abadi, Andy Chu, Ian Goodfellow, H. Brendan McMahan, Ilya Mironov, Kunal Talwar, and  
 497 Li Zhang. Deep learning with differential privacy. In *Proceedings of the 2016 ACM SIGSAC  
 498 Conference on Computer and Communications Security*, CCS '16, pp. 308–318, New York, NY,  
 499 USA, 2016. Association for Computing Machinery. ISBN 9781450341394. doi: 10.1145/2976749.  
 500 2978318. URL <https://doi.org/10.1145/2976749.2978318>.

501 Paul Albert, Frederic Z Zhang, Cristian Rodriguez-Opazo, Hemanth Saratchandran, Anton van den  
 502 Hengel, and Ehsan Abbasnejad. Randlora: full rank parameter-efficient fine-tuning of large models.  
 503 *International Conference on Learning Representations (ICLR)*, 2024.

504 Sören Auer, Christian Bizer, Georgi Kobilarov, Jens Lehmann, Richard Cyganiak, and Zachary Ives.  
 505 Dbpedia: A nucleus for a web of open data. In Karl Aberer, Key-Sun Choi, Natasha Noy, Dean  
 506 Allemang, Kyung-Il Lee, Lyndon Nixon, Jennifer Golbeck, Peter Mika, Diana Maynard, Riichiro  
 507 Mizoguchi, Guus Schreiber, and Philippe Cudré-Mauroux (eds.), *The Semantic Web*, pp. 722–735,  
 508 Berlin, Heidelberg, 2007. Springer Berlin Heidelberg. ISBN 978-3-540-76298-0.

509 Massimo Bini, Leander Girrbach, and Zeynep Akata. Decoupling angles and strength in low-rank  
 510 adaptation. In *International Conference on Learning Representations (ICLR)*, 2025.

512 Rickard Brüel-Gabrielsson, Jiacheng Zhu, Onkar Bhardwaj, Leshem Choshen, Kristjan Greenewald,  
 513 Mikhail Yurochkin, and Justin Solomon. Compress then serve: Serving thousands of lora adapters  
 514 with little overhead, 2024. URL <https://arxiv.org/abs/2407.00066>.

515 Eric L. Buehler and Markus J. Buehler. X-lora: Mixture of low-rank adapter experts, a flexible  
 516 framework for large language models with applications in protein mechanics and molecular design.  
 517 *APL Machine Learning*, 2(2):026119, 05 2024. ISSN 2770-9019. doi: 10.1063/5.0203126. URL  
 518 <https://doi.org/10.1063/5.0203126>.

520 Lucas Caccia, Edoardo Ponti, Zhan Su, Matheus Pereira, Nicolas Le Roux, and Alessandro Sordoni.  
 521 Multi-head adapter routing for cross-task generalization. In *Thirty-seventh Conference on Neural  
 522 Information Processing Systems*, 2023. URL <https://openreview.net/forum?id=qcQhBli5Ho>.

524 Nicholas Carlini, Steve Chien, Milad Nasr, Shuang Song, Andreas Terzis, and Florian Tramèr.  
 525 Membership inference attacks from first principles. In *2022 IEEE Symposium on Security and  
 526 Privacy (SP)*, pp. 1897–1914, 2022. doi: 10.1109/SP46214.2022.9833649.

527 Somnath Basu Roy Chowdhury, Krzysztof Marcin Choromanski, Arijit Sehanobish, Kumar Avinava  
 528 Dubey, and Snigdha Chaturvedi. Towards scalable exact machine unlearning using parameter-  
 529 efficient fine-tuning. In *The Thirteenth International Conference on Learning Representations*,  
 530 2025. URL <https://openreview.net/forum?id=oe51Q5Uo37>.

532 Alexandra Chronopoulou, Matthew Peters, Alexander Fraser, and Jesse Dodge. AdapterSoup: Weight  
 533 averaging to improve generalization of pretrained language models. In Andreas Vlachos and  
 534 Isabelle Augenstein (eds.), *Findings of the Association for Computational Linguistics: EACL  
 535 2023*, pp. 2054–2063, Dubrovnik, Croatia, May 2023. Association for Computational Linguistics.  
 536 doi: 10.18653/v1/2023.findings-eacl.153. URL [https://aclanthology.org/2023.  
 537 findings-eacl.153/](https://aclanthology.org/2023.findings-eacl.153/).

538 William B. Dolan and Chris Brockett. Automatically constructing a corpus of sentential paraphrases.  
 539 In *Proceedings of the Third International Workshop on Paraphrasing (IWP2005)*, 2005. URL  
<https://aclanthology.org/I05-5002/>.

540 Cynthia Dwork and Aaron Roth. The algorithmic foundations of differential privacy. 9(3–4):211–407,  
 541 August 2014. ISSN 1551-305X. doi: 10.1561/0400000042. URL <https://doi.org/10.1561/0400000042>.

543

544 William Fedus, Barret Zoph, and Noam Shazeer. Switch transformers: scaling to trillion parameter  
 545 models with simple and efficient sparsity. 23(1), January 2022. ISSN 1532-4435.

546

547 William Fleshman and Benjamin Van Durme. Lora-augmented generation (lag) for knowledge-  
 548 intensive language tasks, 2025a. URL <https://arxiv.org/abs/2507.05346>.

549

550 William Fleshman and Benjamin Van Durme. Spectr: Dynamically composing lm experts with  
 551 spectral routing, 2025b. URL <https://arxiv.org/abs/2504.03454>.

552

553 William Fleshman, Aleem Khan, Marc Marone, and Benjamin Van Durme. Adapterswap: Continuous  
 554 training of llms with data removal and access-control guarantees. In *Proceedings of Conference  
 555 on Applied Machine Learning in Information Security (CAMLIS) 2024*, 2024. URL <https://arxiv.org/abs/2404.08417>.

556

557 Aaron Grattafiori, Abhimanyu Dubey, Abhinav Jauhri, Abhinav Pandey, Abhishek Kadian, Ahmad  
 558 Al-Dahle, Aiesha Letman, Akhil Mathur, Alan Schelten, Alex Vaughan, Amy Yang, Angela Fan,  
 559 Anirudh Goyal, Anthony Hartshorn, Aobo Yang, Archi Mitra, Archie Sravankumar, Artem Korenev,  
 560 Arthur Hinsvark, Arun Rao, Aston Zhang, Aurelien Rodriguez, Austen Gregerson, Ava Spataru,  
 561 Baptiste Roziere, Bethany Biron, Binh Tang, Bobbie Chern, Charlotte Caucheteux, Chaya Nayak,  
 562 Chloe Bi, Chris Marra, Chris McConnell, Christian Keller, Christophe Touret, Chunyang Wu, et al.  
 563 The llama 3 herd of models, 2024. URL <https://arxiv.org/abs/2407.21783>.

564

565 Pengxin Guo, Shuang Zeng, Yanran Wang, Huijie Fan, Feifei Wang, and Liangqiong Qu. Selective  
 566 aggregation for low-rank adaptation in federated learning. In *The Thirteenth International Confer-  
 567 ence on Learning Representations*, 2025. URL <https://openreview.net/forum?id=iX3uESGdsO>.

568

569 Edward J Hu, yelong shen, Phillip Wallis, Zeyuan Allen-Zhu, Yuanzhi Li, Shean Wang, Lu Wang,  
 570 and Weizhu Chen. LoRA: Low-rank adaptation of large language models. In *International  
 571 Conference on Learning Representations*, 2022. URL <https://openreview.net/forum?id=nZeVKeeFYf9>.

572

573 Chengsong Huang, Qian Liu, Bill Yuchen Lin, Tianyu Pang, Chao Du, and Min Lin. Lorahub: Effi-  
 574 cient cross-task generalization via dynamic loRA composition. In *First Conference on Language  
 575 Modeling*, 2024. URL <https://openreview.net/forum?id=TrloAXEJ2B>.

576

577 Gabriel Ilharco, Marco Túlio Ribeiro, Mitchell Wortsman, Ludwig Schmidt, Hannaneh Hajishirzi,  
 578 and Ali Farhadi. Editing models with task arithmetic. In *The Eleventh International Confer-  
 579 ence on Learning Representations*, 2023. URL <https://openreview.net/forum?id=6t0Kwf8-jrj>.

580

581 Robert Jacobs, Michael Jordan, Steven Nowlan, and Geoffrey Hinton. Adaptive mixtures of local  
 582 experts. *Neural Computation*, 3:79–87, 03 1991. doi: 10.1162/neco.1991.3.1.79.

583

584 Dawid J. Koviczko, Tijmen Blankevoort, and Yuki M. Asano. Vera: Vector-based random matrix  
 585 adaptation. In *The Twelfth International Conference on Learning Representations (ICLR)*, 2024.

586

587 Yang Li, Shaobo Han, and Shihao Ji. VB-loRA: Extreme parameter efficient fine-tuning with vector  
 588 banks. In *The Thirty-eighth Annual Conference on Neural Information Processing Systems*, 2024.  
 589 URL <https://openreview.net/forum?id=kuCY0mW4Q3>.

590

591 Shih-Yang Liu, Chien-Yi Wang, Hongxu Yin, Pavlo Molchanov, Yu-Chiang Frank Wang, Kwang-  
 592 Ting Cheng, and Min-Hung Chen. Dora: Weight-decomposed low-rank adaptation. *CoRR*,  
 593 abs/2402.09353, 2024a. URL <https://doi.org/10.48550/arXiv.2402.09353>.

594

595 Yibing Liu, Chris XING TIAN, Haoliang Li, Lei Ma, and Shiqi Wang. Neuron activation coverage:  
 596 Rethinking out-of-distribution detection and generalization. In *The Twelfth International Confer-  
 597 ence on Learning Representations*, 2024b. URL <https://openreview.net/forum?id=SNGXbZtK6Q>.

594 Sourab Mangrulkar, Sylvain Gugger, Lysandre Debut, Younes Belkada, Sayak Paul, and Benjamin  
 595 Bossan. Peft: State-of-the-art parameter-efficient fine-tuning methods. <https://github.com/huggingface/peft>, 2022.

596

597 Guillermo Ortiz-Jimenez, Alessandro Favero, and Pascal Frossard. Task arithmetic in the tangent  
 598 space: Improved editing of pre-trained models. In *Thirty-seventh Conference on Neural Information  
 599 Processing Systems*, 2023. URL <https://openreview.net/forum?id=0A9f2jZDGW>.

600

601 Oleksiy Ostapenko, Zhan Su, Edoardo Ponti, Laurent Charlin, Nicolas Le Roux, Lucas Caccia, and  
 602 Alessandro Sordoni. Towards modular LLMs by building and reusing a library of loRAs. In  
 603 *Forty-first International Conference on Machine Learning*, 2024. URL <https://openreview.net/forum?id=0ZFWfeVsaD>.

604

605 Jaewoo Park, Jacky Chen Long Chai, Jaeho Yoon, and Andrew Beng Jin Teoh. Understanding the  
 606 feature norm for out-of-distribution detection. In *2023 IEEE/CVF International Conference on  
 607 Computer Vision (ICCV)*, pp. 1557–1567, 2023. doi: 10.1109/ICCV51070.2023.00150.

608

609 Jonas Pfeiffer, Aishwarya Kamath, Andreas Rücklé, Kyunghyun Cho, and Iryna Gurevych. Adapter-  
 610 Fusion: Non-destructive task composition for transfer learning. In Paola Merlo, Jorg Tiede-  
 611 mann, and Reut Tsarfaty (eds.), *Proceedings of the 16th Conference of the European Chapter  
 612 of the Association for Computational Linguistics: Main Volume*, pp. 487–503, Online, April  
 613 2021. Association for Computational Linguistics. doi: 10.18653/v1/2021.eacl-main.39. URL  
 614 <https://aclanthology.org/2021.eacl-main.39>.

615 Edoardo Maria Ponti, Alessandro Sordoni, Yoshua Bengio, and Siva Reddy. Combining parameter-  
 616 efficient modules for task-level generalisation. In Andreas Vlachos and Isabelle Augenstein (eds.),  
 617 *Proceedings of the 17th Conference of the European Chapter of the Association for Computational  
 618 Linguistics*, pp. 687–702, Dubrovnik, Croatia, May 2023. Association for Computational Lin-  
 619 guistics. doi: 10.18653/v1/2023.eacl-main.49. URL <https://aclanthology.org/2023.eacl-main.49>.

620

621 Qwen, An Yang, Baosong Yang, Beichen Zhang, Binyuan Hui, Bo Zheng, Bowen Yu, Chengyuan  
 622 Li, Dayiheng Liu, Fei Huang, Haoran Wei, Huan Lin, Jian Yang, Jianhong Tu, Jianwei Zhang,  
 623 Jianxin Yang, Jiaxi Yang, Jingren Zhou, Junyang Lin, Kai Dang, Keming Lu, Keqin Bao, Kexin  
 624 Yang, Le Yu, Mei Li, Mingfeng Xue, Pei Zhang, Qin Zhu, Rui Men, Runji Lin, Tianhao Li, Tianyi  
 625 Tang, Tingyu Xia, Xingzhang Ren, Xuancheng Ren, Yang Fan, Yang Su, Yichang Zhang, Yu Wan,  
 626 Yuqiong Liu, Zeyu Cui, Zhenru Zhang, and Zihan Qiu. Qwen2.5 technical report, 2025. URL  
 627 <https://arxiv.org/abs/2412.15115>.

628

629 Pranav Rajpurkar, Jian Zhang, Konstantin Lopyrev, and Percy Liang. SQuAD: 100,000+ questions  
 630 for machine comprehension of text. In Jian Su, Kevin Duh, and Xavier Carreras (eds.), *Proceedings  
 631 of the 2016 Conference on Empirical Methods in Natural Language Processing*, pp. 2383–2392,  
 632 Austin, Texas, November 2016. Association for Computational Linguistics. doi: 10.18653/v1/  
 633 D16-1264. URL <https://aclanthology.org/D16-1264>.

634

635 Weijia Shi, Akshita Bhagia, Kevin Farhat, Niklas Muennighoff, Pete Walsh, Jacob Morrison, Dustin  
 636 Schwenk, Shayne Longpre, Jake Poznanski, Allyson Ettinger, Daogao Liu, Margaret Li, Dirk  
 637 Groeneveld, Mike Lewis, Wen tau Yih, Luca Soldaini, Kyle Lo, Noah A. Smith, Luke Zettlemoyer,  
 638 Pang Wei Koh, Hannaneh Hajishirzi, Ali Farhadi, and Sewon Min. Flexolmo: Open language  
 639 models for flexible data use, 2025. URL <https://arxiv.org/abs/2507.07024>.

640

641 Dong Geun Shin and Hye Won Chung. Representation norm amplification for out-of-distribution  
 642 detection in long-tail learning, 2024. URL <https://arxiv.org/abs/2408.10676>.

643

644 Reza Shokri, Marco Stronati, Congzheng Song, and Vitaly Shmatikov. Membership Inference Attacks  
 645 Against Machine Learning Models . In *2017 IEEE Symposium on Security and Privacy (SP)*, pp.  
 646 3–18, Los Alamitos, CA, USA, May 2017. IEEE Computer Society. doi: 10.1109/SP.2017.41.  
 647 URL <https://doi.ieeecomputersociety.org/10.1109/SP.2017.41>.

648

649 Richard Socher, Alex Perelygin, Jean Wu, Jason Chuang, Christopher D. Manning, Andrew Ng, and  
 650 Christopher Potts. Recursive deep models for semantic compositionality over a sentiment treebank.  
 651 In David Yarowsky, Timothy Baldwin, Anna Korhonen, Karen Livescu, and Steven Bethard (eds.),

648 *Proceedings of the 2013 Conference on Empirical Methods in Natural Language Processing*, pp.  
649 1631–1642, Seattle, Washington, USA, October 2013. Association for Computational Linguistics.  
650 URL <https://aclanthology.org/D13-1170/>.

651 George Stoica, Pratik Ramesh, Boglarka Ecsedi, Leshem Choshen, and Judy Hoffman. Model  
652 merging with SVD to tie the knots. In *The Thirteenth International Conference on Learning  
653 Representations*, 2025. URL <https://openreview.net/forum?id=67X93aZHII>.

654 Mingjie Sun, Xinlei Chen, J Zico Kolter, and Zhuang Liu. Massive activations in large language  
655 models. In *First Conference on Language Modeling*, 2024a. URL [https://openreview.net/forum?id=F7aAhfitX6](https://openreview.net/forum?<br/>
656 id=F7aAhfitX6).

657 Youbang Sun, Zitao Li, Yaliang Li, and Bolin Ding. Improving LoRA in privacy-preserving federated  
658 learning. In *The Twelfth International Conference on Learning Representations*, 2024b. URL  
659 <https://openreview.net/forum?id=NLPzL6HWN1>.

660 Anke Tang, Li Shen, Yong Luo, Yibing Zhan, Han Hu, Bo Du, Yixin Chen, and Dacheng Tao.  
661 Parameter-efficient multi-task model fusion with partial linearization. In *The Twelfth International  
662 Conference on Learning Representations*, 2024. URL [https://openreview.net/forum?id=iynRvVVAmH](https://openreview.net/forum?<br/>
663 id=iynRvVVAmH).

664 Weilin Wan, Weizhong Zhang, Quan Zhou, Fan Yi, and Cheng Jin. Out-of-distribution detection  
665 using neural activation prior, 2024. URL <https://arxiv.org/abs/2402.18162>.

666 Alex Wang, Amanpreet Singh, Julian Michael, Felix Hill, Omer Levy, and Samuel Bowman. GLUE:  
667 A multi-task benchmark and analysis platform for natural language understanding. In Tal Linzen,  
668 Grzegorz Chrupa  , and Afra Alishahi (eds.), *Proceedings of the 2018 EMNLP Workshop Black-  
669 boxNLP: Analyzing and Interpreting Neural Networks for NLP*, pp. 353–355, Brussels, Belgium,  
670 November 2018. Association for Computational Linguistics. doi: 10.18653/v1/W18-5446. URL  
671 [https://aclanthology.org/W18-5446/](https://aclanthology.org/W18-5446).

672 Yaqing Wang, Sahaj Agarwal, Subhabrata Mukherjee, Xiaodong Liu, Jing Gao, Ahmed Hassan  
673 Awadallah, and Jianfeng Gao. AdaMix: Mixture-of-adaptations for parameter-efficient model  
674 tuning. In Yoav Goldberg, Zornitsa Kozareva, and Yue Zhang (eds.), *Proceedings of the 2022 Con-  
675 ference on Empirical Methods in Natural Language Processing*, pp. 5744–5760, Abu Dhabi, United  
676 Arab Emirates, December 2022. Association for Computational Linguistics. doi: 10.18653/v1/  
677 2022.emnlp-main.388. URL [https://aclanthology.org/2022.emnlp-main.388/](https://aclanthology.org/2022.emnlp-main.388).

678 Alex Warstadt, Amanpreet Singh, and Samuel R. Bowman. Neural network acceptability judgments.  
679 *Transactions of the Association for Computational Linguistics*, 7:625–641, 2019. doi: 10.1162/  
680 tacl\_a\_00290. URL <https://aclanthology.org/Q19-1040/>.

681 Adina Williams, Nikita Nangia, and Samuel Bowman. A broad-coverage challenge corpus for  
682 sentence understanding through inference. In Marilyn Walker, Heng Ji, and Amanda Stent  
683 (eds.), *Proceedings of the 2018 Conference of the North American Chapter of the Association  
684 for Computational Linguistics: Human Language Technologies, Volume 1 (Long Papers)*, pp.  
685 1112–1122, New Orleans, Louisiana, June 2018. Association for Computational Linguistics. doi:  
686 10.18653/v1/N18-1101. URL [https://aclanthology.org/N18-1101/](https://aclanthology.org/N18-1101).

687 Thomas Wolf, Lysandre Debut, Victor Sanh, Julien Chaumond, Clement Delangue, Anthony Moi,  
688 Pierric Cistac, Tim Rault, R  mi Louf, Morgan Funtowicz, Joe Davison, Sam Shleifer, Patrick von  
689 Platen, Clara Ma, Yacine Jernite, Julien Plu, Canwen Xu, Teven Le Scao, Sylvain Gugger, Mariama  
690 Drame, Quentin Lhoest, and Alexander M. Rush. Huggingface’s transformers: State-of-the-art  
691 natural language processing, 2020. URL <https://arxiv.org/abs/1910.03771>.

692 Mitchell Wortsman, Gabriel Ilharco, Samir Ya Gadre, Rebecca Roelofs, Raphael Gontijo-Lopes,  
693 Ari S Morcos, Hongseok Namkoong, Ali Farhadi, Yair Carmon, Simon Kornblith, and Ludwig  
694 Schmidt. Model soups: averaging weights of multiple fine-tuned models improves accuracy without  
695 increasing inference time. In Kamalika Chaudhuri, Stefanie Jegelka, Le Song, Csaba Szepesvari,  
696 Gang Niu, and Sivan Sabato (eds.), *Proceedings of the 39th International Conference on Machine  
697 Learning*, volume 162 of *Proceedings of Machine Learning Research*, pp. 23965–23998. PMLR, 17–  
698 23 Jul 2022. URL <https://proceedings.mlr.press/v162/wortsman22a.html>.

702 Prateek Yadav, Derek Tam, Leshem Choshen, Colin Raffel, and Mohit Bansal. TIES-merging:  
 703 Resolving interference when merging models. In *Thirty-seventh Conference on Neural Information  
 704 Processing Systems*, 2023. URL <https://openreview.net/forum?id=xtaX3WyCj1>.  
 705

706 Dixi Yao. Risks when sharing lora fine-tuned diffusion model weights, 2024. URL <https://arxiv.org/abs/2409.08482>.  
 707

708 Le Yu, Bowen Yu, Haiyang Yu, Fei Huang, and Yongbin Li. Language models are super mario:  
 709 Absorbing abilities from homologous models as a free lunch. In *ICML*, 2024. URL <https://openreview.net/forum?id=fq0NaiU8Ex>.  
 710

711 Ted Zadouri, Ahmet Üstün, Arash Ahmadian, Beyza Ermis, Acyr Locatelli, and Sara Hooker.  
 712 Pushing mixture of experts to the limit: Extremely parameter efficient moe for instruction tuning.  
 713 In *The Twelfth International Conference on Learning Representations*, 2024. URL <https://openreview.net/forum?id=EvDeiLv7qc>.  
 714

715 Rowan Zellers, Ari Holtzman, Yonatan Bisk, Ali Farhadi, and Yejin Choi. HellaSwag: Can a  
 716 machine really finish your sentence? In Anna Korhonen, David Traum, and Lluís Márquez  
 717 (eds.), *Proceedings of the 57th Annual Meeting of the Association for Computational Linguistics*,  
 718 pp. 4791–4800, Florence, Italy, July 2019. Association for Computational Linguistics. doi:  
 719 10.18653/v1/P19-1472. URL <https://aclanthology.org/P19-1472>.  
 720

721 Longteng Zhang, Lin Zhang, Shaohuai Shi, Xiaowen Chu, and Bo Li. Lora-fa: Memory-efficient  
 722 low-rank adaptation for large language models fine-tuning, 2023a. URL <https://arxiv.org/abs/2308.03303>.  
 723

724 Qingru Zhang, Minshuo Chen, Alexander Bukharin, Pengcheng He, Yu Cheng, Weizhu Chen,  
 725 and Tuo Zhao. Adaptive budget allocation for parameter-efficient fine-tuning. In *The Eleventh  
 726 International Conference on Learning Representations*, 2023b. URL <https://openreview.net/forum?id=1q62uWRJjiY>.  
 727

728 Xin Zhou, Martin Weyssow, Ratnadira Widayarsi, Ting Zhang, Junda He, Yunbo Lyu, Jianming  
 729 Chang, Beiqi Zhang, Dan Huang, and David Lo. Lessleak-bench: A first investigation of data  
 730 leakage in llms across 83 software engineering benchmarks, 2025. URL <https://arxiv.org/abs/2502.06215>.  
 731

732 Jiacheng Zhu, Kristjan Greenewald, Kimia Nadjahi, Haitz Sáez de Ocáriz Borde, Rickard Brüel  
 733 Gabrielsson, Leshem Choshen, Marzyeh Ghassemi, Mikhail Yurochkin, and Justin Solomon.  
 734 Asymmetry in low-rank adapters of foundation models. In *Forty-first International Conference on  
 735 Machine Learning*, 2024. URL <https://openreview.net/forum?id=txRZBD8tBV>.  
 736

737

## A ARROW PROOF

738

739 *Proof.* We will construct 2x2 LoRA adapters  $C$  and  $D$  and an input  $\mathbf{x}$  that satisfy the condition of  
 740 the theorem.

741 1. Define  $C = B_1 A_1$ :

742 Let matrix  $C = \begin{pmatrix} 2 & 0 \\ 0 & 1 \end{pmatrix}$ .

743 The singular values are  $\sigma_1(C) = 2$  and  $\sigma_2(C) = 1$ . The right singular vector corresponding  
 744 to  $\sigma_1$  is  $\mathbf{v}_C = \begin{pmatrix} 1 \\ 0 \end{pmatrix}$ .

745 2. Define  $D = B_2 A_2$ :

746 We construct  $D$  from the singular value decomposition  $D = USV^T$  and choose the  
 747 components to satisfy the theorem.

748 Let  $U = I$  the identity.

756 Let the singular values be  $\sigma_1(D) = 3$  and  $\sigma_2(D) = 1$ .  
 757  
 758 Let the right singular vectors be  $\mathbf{v}_D = \frac{1}{\sqrt{2}} \begin{pmatrix} 1 \\ 1 \end{pmatrix}$  and  $\frac{1}{\sqrt{2}} \begin{pmatrix} 1 \\ -1 \end{pmatrix}$ .  
 759  
 760 
$$D = USV^T = \begin{pmatrix} 1 & 0 \\ 0 & 1 \end{pmatrix} \begin{pmatrix} 3 & 0 \\ 0 & 1 \end{pmatrix} \begin{pmatrix} \frac{1}{\sqrt{2}} & \frac{1}{\sqrt{2}} \\ \frac{1}{\sqrt{2}} & -\frac{1}{\sqrt{2}} \end{pmatrix}^T = \begin{pmatrix} \frac{3}{\sqrt{2}} & \frac{3}{\sqrt{2}} \\ \frac{1}{\sqrt{2}} & -\frac{1}{\sqrt{2}} \end{pmatrix}.$$
  
 761  
 762  
 763

764 3. Choose vector  $\mathbf{x}$ :

765 Let  $\mathbf{x} = \mathbf{v}_C = \begin{pmatrix} 1 \\ 0 \end{pmatrix}$ .  
 766  
 767

768 4. Verify inequality:

769  
 770  
 771 
$$LHS = \operatorname{argmax}_i |\mathbf{v}_i^T \mathbf{x}|$$
  
 772  
 773  $= \operatorname{argmax}_i \{ |\mathbf{v}_C^T \mathbf{x}|, |\mathbf{v}_D^T \mathbf{x}| \}$   
 774  
 775  $= \operatorname{argmax}_i \{ 1, \frac{1}{\sqrt{2}} \} = (\text{adapter 1}).$   
 776  
 777

778 
$$RHS = \operatorname{argmax}_i \|B_i A_i \mathbf{x}\|_2$$
  
 779  
 780  $= \operatorname{argmax}_i \{ \|C \mathbf{x}\|_2, \|D \mathbf{x}\|_2 \}$   
 781  
 782  $= \operatorname{argmax}_i \{ \left\| \begin{pmatrix} 2 \\ 0 \end{pmatrix} \right\|_2, \left\| \begin{pmatrix} \frac{3}{\sqrt{2}} \\ \frac{1}{\sqrt{2}} \end{pmatrix} \right\|_2 \}$   
 783  
 784  $= \operatorname{argmax}_i \{ 2, \sqrt{5} \} = (\text{adapter 2}).$   
 785

786  $LHS \neq RHS.$

787  
 788  
 789  
 790  $\square$   
 791

## B SPECTR PROOF

794 *Proof.* Let  $B \in \mathbb{R}^{m \times r}$ ,  $A \in \mathbb{R}^{r \times n}$ , and  $\mathbf{x} \in \mathbb{R}^n$ . So,

795 
$$\|BA\mathbf{x}\|_2 = \|USV^T \mathbf{x}\|_2 \quad (\text{Equation 1})$$

796  $= \|U\hat{A}\mathbf{x}\|_2 \quad (\text{Equation 3})$

797  $= \sqrt{\|U\hat{A}\mathbf{x}\|_2^2}$

798  $= \sqrt{\mathbf{x}^T \hat{A}^T U^T U \hat{A} \mathbf{x}} \quad (\text{Definition of squared 2-norm})$

799  $= \sqrt{\mathbf{x}^T \hat{A}^T \hat{A} \mathbf{x}} \quad (\text{Orthonormal columns} \implies U^T U = I)$

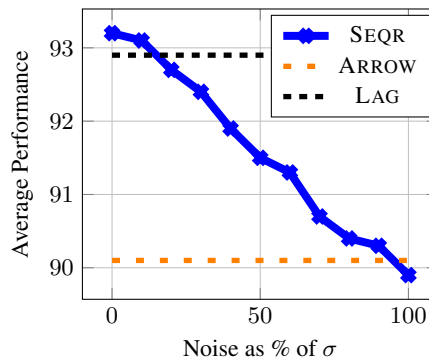
800  $= \sqrt{\|\hat{A}\mathbf{x}\|_2^2}$

801  $= \|\hat{A}\mathbf{x}\|_2$

802  
 803  
 804  
 805  
 806  
 807  
 808  
 809  $\square$

810  
811 C SEQR PROOF812 *Proof.* Let  $B \in \mathbb{R}^{m \times r}$ ,  $A \in \mathbb{R}^{r \times n}$ ,  $\mathbf{x} \in \mathbb{R}^n$ , and  $B = QR$  from Equation 4. So,

$$\begin{aligned}
 814 \quad \|BA\mathbf{x}\|_2 &= \|QR\mathbf{x}\|_2 && \text{(substitution)} \\
 815 \quad &= \sqrt{\|QR\mathbf{x}\|_2^2} \\
 816 \quad &= \sqrt{\mathbf{x}^T A^T R^T Q^T Q R \mathbf{x}} \\
 817 \quad &= \sqrt{\mathbf{x}^T A^T R^T R \mathbf{x}} && \text{(Orthonormal columns} \implies Q^T Q = I) \\
 818 \quad &= \sqrt{\|R\mathbf{x}\|_2^2} \\
 819 \quad &= \|R\mathbf{x}\|_2 \\
 820 \quad &= \|R\mathbf{x}\|_2 \\
 821 \quad &= \|R\mathbf{x}\|_2 \\
 822 \quad &= \|R\mathbf{x}\|_2
 \end{aligned}$$

823  
824  $\square$   
825  
826827 D ADAPTER DETAILS  
828829 We fit LoRA adapters targeting all attention layers in the network (query, key, value, and output  
830 projection layers). We choose initial settings for the LoRAs using the unsloth hyperparameter  
831 guide.<sup>6</sup> We use rank-32 adapters with a LoRA  $\alpha = 64$  and dropout of 0.05. We train for two epochs  
832 using a cosine schedule with warm-up ratio of 5% and a batch size of 8. We sweep learning rates in  
833 the set  $\{5e-6, 1e-5, 2e-5, 5e-5, 1e-4, 2e-4, 5e-4, 1e-3, 2e-3, 5e-3\}$  for each dataset, but share learning  
834 rates across random seeds. We provide our source code for ease of replication.  
835836 E NORM ROBUSTNESS  
837838 SEQR scores use the estimated mean and standard deviation of the activation norms seen in the  
839 training data. We measure how sensitive the performance of SEQR is with respect to these estimates.  
840 We evaluate over our entire testing dataset, adding noise to the estimated means before z-scoring.  
841 The noise simulates post-calibration distribution shift or a noisy estimation of the mean activations  
842 during calibration. We add gaussian noise with varying intensities to alter the means by up to a full  
843 standard deviation of the activation distribution. Figure 6 displays the average performance of SEQR  
844 as noise is added. SEQR is robust to estimation errors, and falls below the performance of LAG and  
845 ARROW only when the estimated statistics are significantly off (20% and 100% of  $\sigma$  respectively).  
846859 Figure 6: Average performance of SEQR as noise is added to the calibrated activation norm means  
860 with varying intensities.  
861862  
863 <sup>6</sup><https://docs.unsloth.ai/get-started/fine-tuning-llms-guide/lora-hyperparameters-guide>

864 F SEQR ALGORITHM  
865866 We present the complete SEQR procedure in [Algorithm 1](#).  
867868 **Algorithm 1** Secure and Efficient QR (SEQR) Routing  
869

---

870 **Require:** Pretrained weight matrix  $W \in \mathbb{R}^{m \times n}$   
 871    Shared adapter matrix  $A \in \mathbb{R}^{r \times n}$   $\triangleright$  Randomly initialized and frozen during training  
 872    LoRA matrices  $\{B_i \in \mathbb{R}^{m \times r}\}_{i=1}^N$   
 873    Norm statistics  $\{\mu_i, \sigma_i\}_{i=1}^N$   $\triangleright$  Estimated using training data

874 **Preprocessing**  
 875    **for** each adapter  $B_i$  **do**  
 876      Compute reduced QR decomposition:  $B_i = Q_i R_i$   $\triangleright B_i$  can be discarded  
 877    **end for**

878 **Inference** (given input  $\mathbf{x} \in \mathbb{R}^n$ )  
 879    Compute shared intermediate representation:  $\mathbf{z} \leftarrow A\mathbf{x}$   
 880    **for** each adapter  $i = 1, \dots, N$  **do**  
 881      Projected activation:  $\mathbf{h}_i \leftarrow R_i \mathbf{z}$   
 882      Score:  $s_i \leftarrow (\|\mathbf{h}_i\|_2 - \mu_i) / \sigma_i$   $\triangleright$  Z-scored activation norm  
 883    **end for**  
 884    Select top adapter:  $i^* \leftarrow \arg \max_i s_i$   $\triangleright$  Adapter with max activation norm  
 885    Compute final output:  $\mathbf{y} \leftarrow W\mathbf{x} + Q_{i^*} \mathbf{h}_{i^*}$   $\triangleright Q_{i^*} \mathbf{h}_{i^*} = B_{i^*} A\mathbf{x}$   
 886    **return**  $\mathbf{y}$

---

889 G ORACLE PERFORMANCE  
890891 We include the raw task performance of each model when using the ground truth adapter. This  
 892 simulates perfect routing, an upper bound on expected performance. All scores in [Section 4](#) are  
 893 normalized by these values to control for differences in task difficulty or model capability.  
 894895 Table 4: Performance using perfect ground truth routing.  
896

	agnews	cola	dbped	hswag	mnli	mrpc	qnli	qqp	rte	sst2	AVG
Qwen-1.5B	90.3	81.1	98.8	80.7	87.0	85.3	83.4	86.3	86.1	91.7	87.1
Llama-3B	90.0	78.9	99.0	81.5	85.7	85.0	85.5	86.3	87.9	92.8	87.3
Qwen-7B	91.2	85.1	98.8	90.5	90.6	86.7	88.5	87.5	92.5	93.9	90.5
Llama-8B	91.3	82.9	98.7	86.9	88.0	86.1	88.3	88.4	91.6	94.0	89.6

902  
903  
904  
905  
906  
907  
908  
909  
910  
911  
912  
913  
914  
915  
916  
917